

BIFURCATION PHENOMENA IN THE PLANE TENSION TEST

By R. HILL

Department of Applied Mathematics and Theoretical Physics,
University of Cambridge, England

and

J. W. HUTCHINSON

Division of Engineering and Applied Physics, Harvard University, Cambridge, MA, U.S.A.

(Received 22nd April 1975)

SUMMARY

A BASIC tensile bifurcation problem is studied. Bifurcations from a state of homogeneous in-plane tension are investigated for an incompressible rectangular block constrained to undergo plane deformations. The sides of the block are traction-free, and it is elongated by a uniform, shear-free, relative displacement of its ends. For a wide class of incrementally-linear, time-independent materials only two instantaneous moduli enter into the analysis. Symmetric and anti-symmetric bifurcations are examined in each of the characteristic regimes of the governing equations (elliptic, parabolic and hyperbolic). Both diffuse modes and localized shearing modes are considered. Lowest bifurcation stresses are computed for essentially the entire range of possible combinations of material properties and geometry. A number of limiting cases are studied in detail, including those for slender and stubby specimens and for specimens which are rigid in shear. Applications to elastic and elastic/plastic solids are discussed.

1. INTRODUCTION

A STANDARD bifurcation problem is formulated for a rectangular block which is constrained to plane deformations and is subjected to tension in one direction. We suppose that a uniform longitudinal displacement of the ends is prescribed, but that no shearing traction is applied. The material is taken to be initially isotropic or orthotropic with respect to the geometric axes, incompressible, and incrementally linear (wholly or piecewise); its constitutive specification after homogeneous extension then involves just two instantaneous moduli, namely μ for shearing parallel to the geometric axes and μ^* for shearing at 45° to them. A wide range of material response is thus encompassed with a minimum number of parameters, so that the problem lends itself to a thorough study aimed at documenting the variety of possible bifurcations.

To gain perspective we begin by reviewing the theoretical basis in some generality, going beyond the pioneering work of BIOT (1965). In particular, we give prominence to regimes of the stress and moduli that correspond to the elliptic, parabolic, or hyperbolic classifications of the field equations. The extent to which such a framework is significant for understanding bifurcation phenomena is one of our main objectives.

Critical loads are computed over the complete range of moduli and geometry, allowing for competition between full sets of both symmetric and anti-symmetric

modes. We take account also of the possibility of bifurcation by layer deformation (shear bands). The total picture turns out to be much more complicated than might be supposed from the preliminary investigation of the problem by ARIARATNAM and DUBEY (1969).

When $\mu/\mu^* > 2$ we find that bifurcation first becomes possible within the elliptic regime; further, that it is delayed somewhat beyond the load maximum, as observed by HUTCHINSON and MILES (1974) in the analogous axi-symmetric problem for elastic/plastic solids. But, when $\mu/\mu^* < 2$, we find that an infinite number of bifurcations precede the load maximum and are located in the parabolic regime, with points of accumulation on its interface with the elliptic regime.

For a rigid/plastic solid, treated on its merits, there is only a hyperbolic regime. We re-analyse this problem and amplify the results of COWPER and ONAT (1962), aided by the perspective afforded by the present computations in the limit $\mu/\mu^* \rightarrow \infty$.

2. CONSTITUTIVE RELATIONS

Incompressible, time-independent materials are considered which are initially homogeneous and orthotropic (possibly isotropic) with respect to directions of the coordinates x_1, x_2, x_3 in some ground state. The subsequent deformation is maintained plane with in-plane loading coaxial to the directions x_1, x_2 . Up to the instant of bifurcation the boundary-value problems considered here are such that the material remains homogeneous with principal stretches $(\lambda, 1/\lambda)$ from the ground state. The rate equations governing arbitrary in-plane straining at any stage up to bifurcation retain the orthotropic symmetry. Assume, further, that hydrostatic pressure does not influence the constitutive relation between the deviators of stress-rate and strain-rate. Then, for 'incrementally-linear' solids, these relations necessarily have the following structure (as first noted in this context by BIOT (1965, p. 101)):

$$\frac{\mathcal{D}}{\mathcal{D}t}(\sigma_{11} - \sigma_{22}) = 2\mu^*(\varepsilon_{11} - \varepsilon_{22}), \quad \frac{\mathcal{D}}{\mathcal{D}t}\sigma_{12} = 2\mu\varepsilon_{12}, \quad \varepsilon_{11} + \varepsilon_{22} = 0, \quad (2.1)$$

where ε_{ij} is the Eulerian strain-rate, σ_{ij} is the Cauchy stress, and $\mathcal{D}/\mathcal{D}t$ is the Jaumann derivative. In general the instantaneous shear moduli μ and μ^* depend on the deformation history; however, for special materials they may depend on λ alone. When $\mu^* = \mu$ for some λ the moduli will be said to have in-plane 'incremental isotropy' at that instant. The tangent modulus in an in-plane uniaxial test along either x_1 or x_2 is $4\mu^*$; a load maximum is attained when this tangent modulus falls to the current stress value.

For a finitely-elastic rubber-like material which is isotropic with strain energy $W(\lambda)$ per unit ground-state volume,

$$\left. \begin{aligned} 2\mu &= \frac{\lambda^4 + 1}{\lambda^4 - 1}(\sigma_1 - \sigma_2), & 4\mu^* &= \lambda \frac{d}{d\lambda}(\sigma_1 - \sigma_2), \\ \text{with} & & \sigma_1 - \sigma_2 &= \lambda \frac{dW}{d\lambda}, \end{aligned} \right\} \quad (2.2)$$

where σ_1, σ_2 are principal stresses along x_1, x_2 . In an in-plane uniaxial test, a load maximum occurs when $d^2W/d\lambda^2 = 0$. In any history, μ^* vanishes when the maximum

stress difference is attained, where also $\lambda d^2W/d\lambda^2 = -dW/d\lambda$. The Mooney-Rivlin material provides a simple example of stretch-dependent moduli. For this material,

$$W = \frac{1}{2}\mu_0(\lambda^2 + \lambda^{-2} - 2), \quad \sigma_1 - \sigma_2 = \mu_0(\lambda^2 - \lambda^{-2}), \quad \mu^* = \mu = \frac{1}{2}\mu_0(\lambda^2 + \lambda^{-2}),$$

where μ_0 is the ground-state shear modulus. Hence this material has in-plane incremental isotropy at all strains (and likewise if the pre-strain were to include a stretch component along x_3). BIOT (1965, p. 103) proved conversely that this is the only elastic material with this property.

For metals deformed into the plastic range, (2.1) can also represent the elastic (unloading) branch. Then the moduli μ and μ^* are not given by (2.2), however, and are likely to vary only slowly with λ ; no specific dependence is proposed here. When the current yield surface is locally smooth, (2.1) can also represent the plastic (loading) branch, viz. $\varepsilon_{11} > 0$ supposing that $\sigma_1 > \sigma_2$. In that case, continuity demands that the modulus for shearing parallel to the coordinate axes has the same value μ in both branches. On the other hand, the modulus for shearing at 45° to the coordinate axes has different values μ^* and μ_* , say; the usual strain-hardening parameter h , associated with the Jaumann flux, is then given by

$$\frac{1}{h} = \frac{1}{2} \left(\frac{1}{\mu^*} - \frac{1}{\mu_*} \right).$$

When λ is varied monotonically, h and μ^* decrease rapidly but μ_* changes slowly. If the unloading branch is assumed to be isotropic (as tacitly assumed by ARIARATNAM and DUBEY (1969)) then $\mu_* = \mu$.

The structure of the incremental relations (2.1) is preserved under transformation to other objective stress-rates. For the family of fluxes introduced by HILL (1968) one has in the present situation,

$$\left. \begin{aligned} \frac{\mathcal{D}^{(m)}}{\mathcal{D}t} \sigma_{11} &= \frac{\mathcal{D}}{\mathcal{D}t} \sigma_{11} - 2m\sigma_1 \varepsilon_{11}, & \frac{\mathcal{D}^{(m)}}{\mathcal{D}t} \sigma_{22} &= \frac{\mathcal{D}}{\mathcal{D}t} \sigma_{22} - 2m\sigma_2 \varepsilon_{22}, \\ \frac{\mathcal{D}^{(m)}}{\mathcal{D}t} \sigma_{12} &= \frac{\mathcal{D}}{\mathcal{D}t} \sigma_{12} - m(\sigma_1 + \sigma_2)\varepsilon_{12}, \end{aligned} \right\} \quad (2.3)$$

where the parameter m can be assigned any positive or negative value. In terms of the m -fluxes the constitutive relations (2.1) become

$$\frac{\mathcal{D}^{(m)}}{\mathcal{D}t} (\sigma_{11} - \sigma_{22}) = 2\mu^*(m)(\varepsilon_{11} - \varepsilon_{22}), \quad \frac{\mathcal{D}^{(m)}}{\mathcal{D}t} \sigma_{12} = 2\mu(m)\varepsilon_{12},$$

where

$$\mu^*(m) - \mu^* = \mu(m) - \mu = -\frac{1}{2}m(\sigma_1 + \sigma_2). \quad (2.4)$$

Whence, both the orthotropic symmetry and incremental isotropy are invariant under transformation, but the magnitudes (and even the signs) of the moduli are relative to the choice of flux.†

† DUBEY (1975, Section V) considers a family of *compressible* materials, each of which is defined by an *isotropic* relation between $\mathcal{D}^{(m)}\sigma_{ij}/\mathcal{D}t$ and ε_{ij} for one (and necessarily only one) value of m . Dubey also considers the incompressible limit corresponding to $\mu^*(m) = \mu(m)$. However, Dubey tacitly takes every $\mu(m) > 0$ (cf. his equation (5.3) and accompanying discussion of other work), in line with his standpoint that each m -value defines a distinct material. Thus, he is not concerned with transformations of the constitutive law for one and the same material, as here, and consequently overlooks the invariant property (2.4).

For setting up the boundary-value problem it is convenient to have an alternative form of (2.1), in terms of the rate-of-change of the nominal stress n_{ij} , based on the current state at stage t . That is, $n_{ij} + \delta n_{ij}$ is the x_j -component of load at stage $t + \delta t$ on an embedded plane element which was perpendicular to the x_i -axis at stage t and had unit area then. Specialized to the present situation,

$$\left. \begin{aligned} \dot{n}_{11} &= \frac{\mathcal{D}}{\mathcal{D}t} \sigma_{11} - \sigma_1 \frac{\partial v_1}{\partial x_1}, & \dot{n}_{22} &= \frac{\mathcal{D}}{\mathcal{D}t} \sigma_{22} - \sigma_2 \frac{\partial v_2}{\partial x_2}, \\ \dot{n}_{12} &= \frac{\mathcal{D}}{\mathcal{D}t} \sigma_{12} - \frac{1}{2}(\sigma_1 + \sigma_2) \frac{\partial v_1}{\partial x_2} + \frac{1}{2}(\sigma_1 - \sigma_2) \frac{\partial v_2}{\partial x_1}, \\ \dot{n}_{21} &= \frac{\mathcal{D}}{\mathcal{D}t} \sigma_{21} - \frac{1}{2}(\sigma_1 - \sigma_2) \frac{\partial v_1}{\partial x_2} - \frac{1}{2}(\sigma_1 + \sigma_2) \frac{\partial v_2}{\partial x_1}, \end{aligned} \right\} \quad (2.5)$$

where (v_1, v_2) are the (x_1, x_2) -components of velocity. Note that the equation

$$\dot{n}_{12} - \dot{n}_{21} = \sigma_1 \frac{\partial v_2}{\partial x_1} - \sigma_2 \frac{\partial v_1}{\partial x_2}$$

is the statement of continuing rotational equilibrium. Now the Jaumann fluxes in (2.5) may be eliminated using (2.1) with the result

$$\left. \begin{aligned} \dot{n}_{11} - \dot{n}_{22} &= \{2\mu^* - \frac{1}{2}(\sigma_1 + \sigma_2)\} \left(\frac{\partial v_1}{\partial x_1} - \frac{\partial v_2}{\partial x_2} \right), \\ \dot{n}_{12} &= \{ \mu + \frac{1}{2}(\sigma_1 - \sigma_2) \} \frac{\partial v_2}{\partial x_1} + \{ \mu - \frac{1}{2}(\sigma_1 + \sigma_2) \} \frac{\partial v_1}{\partial x_2}, \\ \dot{n}_{21} &= \{ \mu - \frac{1}{2}(\sigma_1 + \sigma_2) \} \frac{\partial v_2}{\partial x_1} + \{ \mu - \frac{1}{2}(\sigma_1 - \sigma_2) \} \frac{\partial v_1}{\partial x_2}. \end{aligned} \right\} \quad (2.6)$$

BIOT (1965, p. 86) calls $\mu - \frac{1}{2}(\sigma_1 - \sigma_2)$ and $\mu + \frac{1}{2}(\sigma_1 - \sigma_2)$ 'slide moduli' since they govern the increment of active nominal load in simple shearing parallel to the (x_1, x_2) -axes respectively. Biot did not use the nominal stress as such but he arrived at the same interpretation indirectly via his peculiar 'symmetrized stress' (which is conjugate to the stretch measure of strain, as expounded by HILL (1968, Appendix)).

The structural symmetry of (2.1), and hence of (2.6), is such that the latter can be combined in a simple variational formula:

$$\dot{n}_{ij} \delta \left(\frac{\partial v_j}{\partial x_i} \right) = \delta U \quad (2.7)$$

subject to the incompressibility restriction ($i, j = 1, 2$ with the summation convention). The function U can be written shortly as

$$U = \frac{1}{2} \dot{n}_{ij} \frac{\partial v_j}{\partial x_i} \quad (2.8)$$

but is to be regarded in (2.7) as expressed in terms of the components of the velocity gradients alone. Explicitly:

$$\begin{aligned} 2U &= 2\{2\mu^* - \frac{1}{2}(\sigma_1 + \sigma_2)\} \left(\frac{\partial v_1}{\partial x_1} \right)^2 + \{ \mu + \frac{1}{2}(\sigma_1 + \sigma_2) \} \left(\frac{\partial v_2}{\partial x_1} \right)^2 \\ &\quad + \{ \mu - \frac{1}{2}(\sigma_1 - \sigma_2) \} \left(\frac{\partial v_1}{\partial x_2} \right)^2 + 2\{ \mu - \frac{1}{2}(\sigma_1 + \sigma_2) \} \frac{\partial v_1}{\partial x_2} \frac{\partial v_2}{\partial x_1}. \end{aligned} \quad (2.9)$$

The terms in U can be combined in a variety of ways, one of the most useful being

$$2U = 2\{2\mu^* - \frac{1}{2}(\sigma_1 + \sigma_2)\} \left(\frac{\partial v_1}{\partial x_1} \right)^2 + \left(\sigma_1 \frac{\partial v_2}{\partial x_1} - \sigma_2 \frac{\partial v_1}{\partial x_2} \right)^2 / (\sigma_1 + \sigma_2) + \frac{1}{2} \left\{ 2\mu - \frac{\sigma_1^2 + \sigma_2^2}{\sigma_1 + \sigma_2} \right\} \left(\frac{\partial v_1}{\partial x_2} + \frac{\partial v_2}{\partial x_1} \right)^2. \quad (2.10)$$

We return to this later in connection with the existence of eigensolutions to boundary-value problems.

3. FIELD EQUATIONS

For continuing linear equilibrium the nominal stress-rate must satisfy $\partial \dot{n}_{ij} / \partial x_i = 0$ or, in a form suited to incompressible materials,

$$\left. \begin{aligned} \frac{\partial}{\partial x_1} \frac{1}{2}(\dot{n}_{11} - \dot{n}_{22}) + \frac{\partial}{\partial x_2} \dot{n}_{21} &= - \frac{\partial}{\partial x_1} \frac{1}{2}(\dot{n}_{11} + \dot{n}_{22}), \\ \frac{\partial}{\partial x_2} \frac{1}{2}(\dot{n}_{11} - \dot{n}_{22}) - \frac{\partial}{\partial x_1} \dot{n}_{12} &= \frac{\partial}{\partial x_2} \frac{1}{2}(\dot{n}_{11} + \dot{n}_{22}). \end{aligned} \right\} \quad (3.1)$$

Differentiate and combine these so as to eliminate $\dot{n}_{11} + \dot{n}_{22}$, which does not appear in the constitutive law. The resulting equation can be expressed entirely in terms of derivatives of the velocities using (2.6). Then, introduce a stream function $\psi(x_1, x_2)$ such that

$$v_1 = \frac{\partial \psi}{\partial x_2}, \quad v_2 = - \frac{\partial \psi}{\partial x_1}. \quad (3.2)$$

On the assumption that the current deviatoric stress is uniform, the result is

$$\{\mu + \frac{1}{2}(\sigma_1 - \sigma_2)\} \frac{\partial^4 \psi}{\partial x_1^4} + 2(2\mu^* - \mu) \frac{\partial^4 \psi}{\partial x_1^2 \partial x_2^2} + \{\mu - \frac{1}{2}(\sigma_1 - \sigma_2)\} \frac{\partial^4 \psi}{\partial x_2^4} = 0. \quad (3.3)$$

Bior's (1965, p. 193) derivation of (3.3) is via equilibrium equations for the Jaumann flux.

Alternatively, we could proceed by introducing a 'stress-rate potential' $\phi(x_1, x_2)$ such that

$$\left. \begin{aligned} \frac{\mathcal{D}}{\mathcal{D}t} \sigma_{11} &= \frac{\partial^2 \phi}{\partial x_2^2}, & \frac{\mathcal{D}}{\mathcal{D}t} \sigma_{22} &= \frac{\partial^2 \phi}{\partial x_1^2}, \\ \frac{\mathcal{D}}{\mathcal{D}t} \sigma_{12} + \frac{1}{2}(\sigma_1 - \sigma_2) \left(\frac{\partial v_2}{\partial x_1} - \frac{\partial v_1}{\partial x_2} \right) &= - \frac{\partial^2 \phi}{\partial x_1 \partial x_2} \end{aligned} \right\} \quad (3.4)$$

in accordance with (2.5) and (3.1), or more immediately by recognizing the left-hand sides of (3.4) as the rates-of-change of Cauchy stress components on the fixed coordinates.

Combine (3.4) with (2.1) and (3.2) to get

$$\left. \begin{aligned} \frac{\partial^2 \phi}{\partial x_2^2} - \frac{\partial^2 \phi}{\partial x_1^2} &= 4\mu^* \frac{\partial^2 \psi}{\partial x_1 \partial x_2}, \\ \frac{\partial^2 \phi}{\partial x_1 \partial x_2} &= \{\mu + \frac{1}{2}(\sigma_1 - \sigma_2)\} \frac{\partial^2 \psi}{\partial x_1^2} - \{\mu - \frac{1}{2}(\sigma_1 - \sigma_2)\} \frac{\partial^2 \psi}{\partial x_2^2}. \end{aligned} \right\} \quad (3.5)$$

In linearized elasticity, with $\sigma_1 = \sigma_2 = 0$, such equations are the basis of a complex

variable formulation; we do not pursue a possible analogous technique here. By eliminating ϕ we recover (3.3), and by eliminating ψ we obtain

$$\{\mu + \frac{1}{2}(\sigma_1 - \sigma_2)\} \frac{\partial^4 \phi}{\partial x_1^4} + 2(2\mu^* - \mu) \frac{\partial^4 \phi}{\partial x_1^2 \partial x_2^2} + \{\mu - \frac{1}{2}(\sigma_1 - \sigma_2)\} \frac{\partial^4 \phi}{\partial x_2^4} = 0. \quad (3.6)$$

Thus, ϕ and ψ satisfy the same differential equation. In the context of a class of elastic/plastic materials, ARIARATNAM and DUBEY (1969) derived (3.6) by another route, without noting (3.5).

Alternatively, we may proceed from the variational principle (HILL, 1958, 1959); see also BIOT (1965, p. 138)):

$$\delta \iint U dx_1 dx_2 = 0 \quad (3.7)$$

for the conventional homogeneous boundary-value problem† for a finite region of the (x_1, x_2) plane. When U is expressed as a function of velocity gradient as in (2.9), or of nominal stress-rate, (3.3) and (3.6) respectively appear as the Euler-Lagrange equation of (3.7).

A condition excluding the possibility of first-order bifurcation in conventional problems for incrementally linear materials is

$$\iint U dx_1 dx_2 > 0 \quad (3.8)$$

for all piecewise-continuously differentiable velocity fields compatible with the constraints (HILL, 1958, 1959). The interpretation of the exclusion condition is that, in any incremental virtual deformation, the loads do less work than is expended internally. In a first-order bifurcation the external and internal works are equal, to second order. Under all-round dead loading the condition is critical in that, when it just fails, a definite first-order bifurcation can be exhibited (HILL, 1967). But under mixed boundary-data of the type considered below, the initial loss of uniqueness may be less simple.

However, the exclusion condition is still informative. For instance, by (2.10), U itself is a positive quadratic in the velocity gradient components if and only if (cf. HILL (1967 (equation 5.4)))

$$0 < \sigma_1 + \sigma_2 < 4\mu^* \quad \text{and} \quad \frac{\sigma_1^2 + \sigma_2^2}{\sigma_1 + \sigma_2} < 2\mu. \quad (3.9)$$

In this range of stress the possibility of first-order bifurcation is therefore ruled out by (3.8), whatever the boundary data. For all-round dead loading, in particular, it was shown by Hill that impending failure of one of these inequalities is in fact critical.

4. CLASSIFICATION OF REGIMES

By way of preparing to solve specific boundary-value problems, we investigate the general character of the differential equation for ϕ and ψ , and its dependence on the current values of the stress and moduli.

† 'Conventional' means that either the velocity or nominal traction-rate vanishes, or else their complementary components vanish over a plane frictionless constraint. If non-planar, a term in its curvature has to be added to (3.7) (cf. BIOT (1965, pp. 143-6)).

Consider any velocity field for which the stream function is of type

$$\psi = F(c_1 x_1 + c_2 x_2), \quad (4.1)$$

where function F is arbitrary and c_1, c_2 are constants. This represents an inhomogeneous simple shear parallel to planes $c_1 x_1 + c_2 x_2 = \text{constant}$. By virtue of the constitutive law every component of any stress-rate deviator is uniform on each such plane, which is to say that all deviator components are annihilated by the operator $(c_1 \partial/\partial x_2 - c_2 \partial/\partial x_1)$. From (3.1), therefore, after multiplying the member equations by c_1 and c_2 respectively,

$$\frac{\partial}{\partial x_1} (c_1 \dot{n}_{11} + c_2 \dot{n}_{21}) = 0, \quad \frac{\partial}{\partial x_2} (c_1 \dot{n}_{12} + c_2 \dot{n}_{22}) = 0.$$

Taken with the preceding statement, these require that

$$c_1 \dot{n}_{11} + c_2 \dot{n}_{21} = c_1 \dot{n}, \quad c_1 \dot{n}_{12} + c_2 \dot{n}_{22} = c_2 \dot{n} \quad (4.2)$$

for general F , where \dot{n} is independent of x_1 and x_2 . The nominal traction-rate over the shearing planes is thus purely normal and of uniform amount \dot{n} . Elimination of this unknown from (4.2) leads to

$$c_1 c_2 (\dot{n}_{11} - \dot{n}_{22}) = c_1^2 \dot{n}_{12} - c_2^2 \dot{n}_{21}.$$

Whence, evaluating the deviator components from (2.6) and (4.1), we must have

$$\{\mu + \frac{1}{2}(\sigma_1 - \sigma_2)\}c_1^4 + 2(2\mu^* - \mu)c_1^2 c_2^2 + \{\mu - \frac{1}{2}(\sigma_1 - \sigma_2)\}c_2^4 = 0 \quad (4.3)$$

for consistency (unless $F(z) \propto z^2$ when c_1/c_2 is arbitrary).

In general there are 2 distinct roots c_1^2/c_2^2 . By combining the 4 associated functions of type (4.1) linearly we obtain a general solution of (3.3). Since we are interested only in real ψ , the character of this solution depends on the *reality or otherwise* of c_1/c_2 . There are three main possibilities, which can be classified as follows under the restrictions

$$\mu^* > 0, \mu > 0, \sigma_1 > \sigma_2: - \quad (4.4)$$

$$E: \text{no real } c_1/c_2, \quad 2\mu^* > \mu - \sqrt{\{\mu^2 - \frac{1}{4}(\sigma_1 - \sigma_2)^2\}}, \quad (4.5)$$

$$H: 4 \text{ real } c_1/c_2, \quad 2\mu^* < \mu - \sqrt{\{\mu^2 - \frac{1}{4}(\sigma_1 - \sigma_2)^2\}}, \quad (4.6)$$

$$P: 2 \text{ real } c_1/c_2, \quad \mu < \frac{1}{2}(\sigma_1 - \sigma_2). \quad (4.7)$$

Symbols $E, H,$ and P stand for elliptic, hyperbolic, and parabolic in conformity with standard terminology for systems of partial differential equations. The corresponding regimes in a plot of $\mu/2\mu^*$ against $(\sigma_1 - \sigma_2)/4\mu^*$ are similarly labeled in Fig. 1; here a point shows directly the degree of incremental anisotropy, and the stress difference relative to the tangent modulus.

The interfaces between regimes E and P , and between H and P , are segments of the line

$$\mu = \frac{1}{2}(\sigma_1 - \sigma_2). \quad (4.8)$$

On this line two roots c_1/c_2 vanish, while the other pair are real along H/P but pure imaginaries along E/P . The interface between E and H is a parabolic arc

$$\frac{\mu}{\mu^*} = 1 + \left(\frac{\sigma_1 - \sigma_2}{4\mu^*}\right)^2 > 2. \quad (4.9)$$

On E/H the roots c_1/c_2 coincide in pairs; in addition to (4.1) there then exist stream

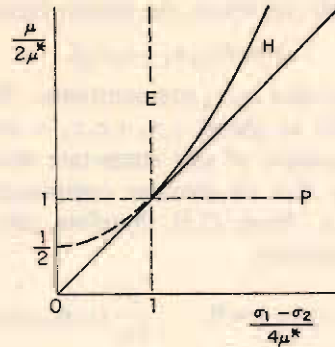


FIG. 1. Characteristic regimes.

functions of type

$$\psi = (c_1 x_1 - c_2 x_2)G(c_1 x_1 + c_2 x_2) \quad (4.10)$$

which are needed to generate a general solution. Note that a further arc of the parabola (shown broken in Fig. 1) divides regime *E* into an upper part where the roots c_1^2/c_2^2 are complex conjugates and a lower part where both are negative (so that all roots c_1/c_2 are pure imaginaries).

The mechanical significance of (4.3) can be appreciated by evaluating the function U in (2.9) at any point of the shearing field (4.1):

$$2U = [\{\mu + \frac{1}{2}(\sigma_1 - \sigma_2)\}c_1^4 + 2(2\mu^* - \mu)c_1^2 c_2^2 + \{\mu - \frac{1}{2}(\sigma_1 - \sigma_2)\}c_2^4] \{F''(c_1 x_1 + c_2 x_2)\}^2.$$

In regime *E* the factor [...] above does not vanish for any real c_1 and c_2 , and is consequently always positive, being so when $c_2 = 0$ by (4.4). Correspondingly, the function U is positive-definite for any incremental simple shear; it is well known that this precludes internal deformation of an incompressible material whose surface is cemented to a rigid container (see, for example, HILL (1962)). In regimes *P* and *H*, on the other hand, the factor [...] is indefinite since it vanishes for either 2 or 4 real values of c_1/c_2 , respectively. Each corresponding line $c_1 x_1 + c_2 x_2 = \text{constant}$ is a characteristic, across which there may be a jump in velocity gradient, amounting to an incremental simple shear in the direction of the line (associated, for example, with a jump in F''). More generally, by setting $\dot{n} = 0$ in (4.2), we see that incremental deformation of type (4.1) can occur inside a layer between any two parallel characteristics, while the loading on momentarily rigid material outside the layer is maintained dead in conformity with zero nominal traction-rate on the layer boundaries.

5. EIGENMODES IN A TENSILE TEST

The specimen is rectangular with current dimensions $2a_1 \times 2a_2$ subject to a current uniaxial stress: $\sigma_1 = \sigma > 0$, $\sigma_2 = 0$. We examine the possibility of incremental deformation when the sides (the faces perpendicular to the x_2 -direction) remain traction-free and the ends are subject to frictionless constraints keeping $v_1 = 0$. We search for modes of the type

$$\psi = v(x_2) \cos(c_1 x_1) \quad (5.1)$$

where, from (3.3), v must satisfy

$$(\mu - \frac{1}{2}\sigma)v'''' - 2(2\mu^* - \mu)c_1^2 v'' + (\mu + \frac{1}{2}\sigma)c_1^4 v = 0. \quad (5.2)$$

Since

$$v_1 = v'(x_2) \cos(c_1 x_1), \quad v_2 = c_1 v(x_2) \sin(c_1 x_1), \quad (5.3)$$

the kinematic constraint on the ends is satisfied when

$$c_1 = m\pi/2a_1, \quad m = 1, 2, \dots, \quad (5.4)$$

by placing the origin of coordinates at the specimen center when m is odd and at a distance a_1/m from the center when m is even. (Alternatively, the origin could be kept central with the case $\psi \propto \sin(c_1 x_1)$ treated separately.)

Since \dot{n}_{12} given by (2.6) also varies as $\cos(c_1 x_1)$, the smoothness condition on the ends is automatically satisfied. On the sides, $\dot{n}_{21} = 0$ if

$$v'' + c_1^2 v = 0, \quad x_2 = \pm a_2, \quad (5.5)$$

while $\dot{n}_{22} = 0$ if

$$(\mu - \frac{1}{2}\sigma)v'''' = (4\mu^* - \mu - \frac{1}{2}\sigma)c_1^2 v', \quad x_2 = \pm a_2. \quad (5.6)$$

The latter can be derived by calculating $\dot{n}_{11} + \dot{n}_{22}$ from (3.1) and setting it equal to $\dot{n}_{11} - \dot{n}_{22}$ in (2.6). Alternatively, the field equation and boundary data for $v(x_2)$ follow from the variational principle (3.7) with free v and v' at the limits, where U is given by (2.9) and (5.3).

Symmetric modes satisfy $\psi(x_1, x_2) = -\psi(x_1, -x_2)$; anti-symmetric modes satisfy $\psi(x_1, x_2) = \psi(x_1, -x_2)$. Hence for the symmetric modes the choice of $v(x_2)$ as an odd function of type

$$v(x_2) = \text{Re} \{A \sin(c_2 x_2)\} \quad (5.7)$$

satisfies (5.2) provided c_2 is any root of

$$(\mu + \frac{1}{2}\sigma)c_1^4 + 2(2\mu^* - \mu)c_1^2 c_2^2 + (\mu - \frac{1}{2}\sigma)c_2^4 = 0 \quad (5.8)$$

in conformity with (4.3). Similarly, anti-symmetric modes are generated by even functions v of the form

$$v(x_2) = \text{Re} \{A \cos(c_2 x_2)\} \quad (5.9)$$

where c_2 must again satisfy (5.8). We now examine the three regimes in turn.

5.1 Elliptic regime

As already observed in connection with (3.9), no modes of any kind exist when

$$0 < \sigma < 2\mu \text{ and } 4\mu^*. \quad (5.10)$$

In Fig. 1 this is that part of region E which is bounded by the E/P interface and the line $\sigma = 4\mu^*$ corresponding to maximum tensile load. Thus, we need only investigate the possibility of modes where the roots c_2^2 are complex conjugates and

$$1 < \frac{\sigma}{4\mu^*} < \sqrt{\left(\frac{\mu}{\mu^*} - 1\right)} \quad \text{and} \quad \mu > 2\mu^*$$

from (4.9). Accordingly, using (5.7) for the symmetric modes, (5.5) and (5.6) can be written as

$$\begin{aligned} \text{Re} [(c_1^2 - c_2^2)A \sin(c_2 a_2)] &= 0, \\ \text{Re} [c_2 A \{(4\mu^* - \mu - \frac{1}{2}\sigma)c_1^2 + (\mu - \frac{1}{2}\sigma)c_2^2\} \cos(c_2 a_2)] &= 0. \end{aligned}$$

The result of eliminating the amplitude factor A can be put as

$$\text{Im} [c_2(c_1^2 - \bar{c}_2^2)^2 \sin(\bar{c}_2 a_2) \cos(c_2 a_2)] = 0.$$

Whence, or by working from the beginning with an explicit real expression for v , we find the eigenvalue equation for the symmetric modes (taking the (+) in (5.11)):

$$\frac{q \sin(2pc_1 a_2)}{p \sinh(2qc_1 a_2)} = \pm \frac{\sqrt{\left(\frac{2\mu - \sigma}{2\mu + \sigma}\right) - \left(1 - \frac{4\mu^*}{\sigma}\right)}}{\sqrt{\left(\frac{2\mu - \sigma}{2\mu + \sigma}\right) + \left(1 - \frac{4\mu^*}{\sigma}\right)}}, \quad (5.11)$$

where

$$p^2 - q^2 = \frac{2\mu - 4\mu^*}{2\mu - \sigma}, \quad p^2 + q^2 = \sqrt{\left(\frac{2\mu + \sigma}{2\mu - \sigma}\right)}. \quad (5.12)$$

Repeating the above calculation for the anti-symmetric modes (5.9) gives (5.11) with (-).

Equations given by ARIARATNAM and DUBEY (1969), and by DUBEY (1975), can be reduced to the above form, which has the merit of combining the parameters in directly meaningful groups.

5.2 Hyperbolic regime

The appropriate real solution for the symmetric modes is

$$v = A \sin(pc_1 x_2) + B \sin(qc_1 x_2),$$

where p and q are now the positive roots c_2/c_1 of (5.8). Elimination of A and B between (5.5) and (5.6) leads to the eigenvalue equation

$$\frac{q \tan(pc_1 a_2)}{p \tan(qc_1 a_2)} = \left(\frac{q^2 - 1}{p^2 - 1}\right)^2, \quad (5.13)$$

where

$$\frac{1}{2}(p^2 + q^2) = \frac{2\mu - 4\mu^*}{2\mu - \sigma}, \quad \frac{1}{2}(p^2 - q^2) = \frac{\sqrt{\{(4\mu^* - 2\mu)^2 + (\sigma^2 - 4\mu^2)\}}}{2\mu - \sigma}. \quad (5.14)$$

For the anti-symmetric modes, v is a linear sum of $\cos(pc_1 x_2)$ and $\cos(qc_1 x_2)$ and the eigenvalue equation is

$$\frac{q \tan(qc_1 a_2)}{p \tan(pc_1 a_2)} = \left(\frac{q^2 - 1}{p^2 - 1}\right)^2. \quad (5.15)$$

The discussion in Section 4 indicates the possibility also of localized shearing deformation in a vanishingly narrow layer, combined with homogeneous extension so as to make v_1 vanish on the ends. For example, a single layer would be geometrically feasible whenever the specimen dimensions are such that a_1/a_2 exceeds the smaller of p and q .

5.3 Parabolic regime

This is not found with finitely-elastic materials (2.2), for which the signs of $\mu \pm \frac{1}{2}(\sigma_1 - \sigma_2)$ always agree, in opposition to (4.4) and (4.7) jointly (cf. BIOT (1965, p. 199)). Generally, however, there are symmetric modes

$$v = A \sin(pc_1 x_2) + B \sinh(qc_1 x_2),$$

where p and iq are respectively the positive and positive-imaginary roots c_2/c_1 .

The eigenvalue equation is

$$\frac{q \tan (pc_1 a_2)}{p \tanh (qc_1 a_2)} = \left(\frac{q^2 + 1}{p^2 - 1} \right)^2, \quad (5.16)$$

where

$$\frac{1}{2}(p^2 - q^2) = \frac{4\mu^* - 2\mu}{\sigma - 2\mu}, \quad \frac{1}{2}(p^2 + q^2) = \frac{\sqrt{\{(4\mu^* - 2\mu)^2 + (\sigma^2 - 4\mu^2)\}}}{\sigma - 2\mu}. \quad (5.17)$$

The eigenvalue equation for the anti-symmetric modes is

$$\frac{q \tanh (qc_1 a_2)}{p \tan (pc_1 a_2)} = - \left(\frac{q^2 + 1}{p^2 - 1} \right)^2. \quad (5.18)$$

Actually, as we shall see later, the E/P interface is a locus of points of accumulation of eigenvalues of (5.16) and (5.18). That is, bifurcations are possible immediately the interface is crossed from E to P , if that is the sense in which the system evolves in parameter space. Some such phenomenon could already be expected from one feature of the behavior of the functional (2.10). This does not comply with (3.8) but takes negative values, however closely σ approaches 2μ from above, for admissible virtual fields $v \propto \sin (cx_2)$ with c sufficiently large; the negative term in $(\partial v_1 / \partial x_2)^2$ is of order c^4 and dominates the integral.

6. BIFURCATION STRESSES IN A TENSION TEST

Our aim in this section is to present a sufficiently complete analysis of the eigenvalue equations listed in Section 5 to reveal the bifurcation stresses for essentially the entire range of material and geometric parameters. Attention is focused on eigenvalues leading to the lowest possible bifurcation stress.

Specialization of (3.9) to in-plane tension ($\sigma_1 = \sigma > 0$, $\sigma_2 = 0$) leads to the pair of implications

$$2\mu^* < \mu \Rightarrow \sigma > 4\mu^*, \quad (6.1)$$

$$2\mu^* > \mu \Rightarrow \sigma > 2\mu. \quad (6.2)$$

From (4.5) to (4.7) it follows that for $2\mu^* < \mu$ the bifurcation stresses may be in any of the three regimes E , H and P , although we will show that the lowest always lies in E . The second case, $2\mu^* > \mu$, implies that any bifurcation stress must fall in P . Case (6.1) is examined first.

6.1 Numerical results ($2\mu^* < \mu$)

Since coincidence of the stress and the tangent modulus $4\mu^*$ corresponds to (possibly local) maximum load, (6.1) ensures that bifurcation cannot occur at stresses below the stress associated with a load maximum. For specified values of $2\mu^*/\mu < 1$ and γ , where

$$\gamma = c_1 a_2 = m\pi a_2 / 2a_1, \quad (6.3)$$

the lowest eigenvalue $\sigma/4\mu^*$ was calculated for the symmetric modes (Fig. 2(a)) and for the anti-symmetric modes (Fig. 2(b)). A standard numerical search procedure

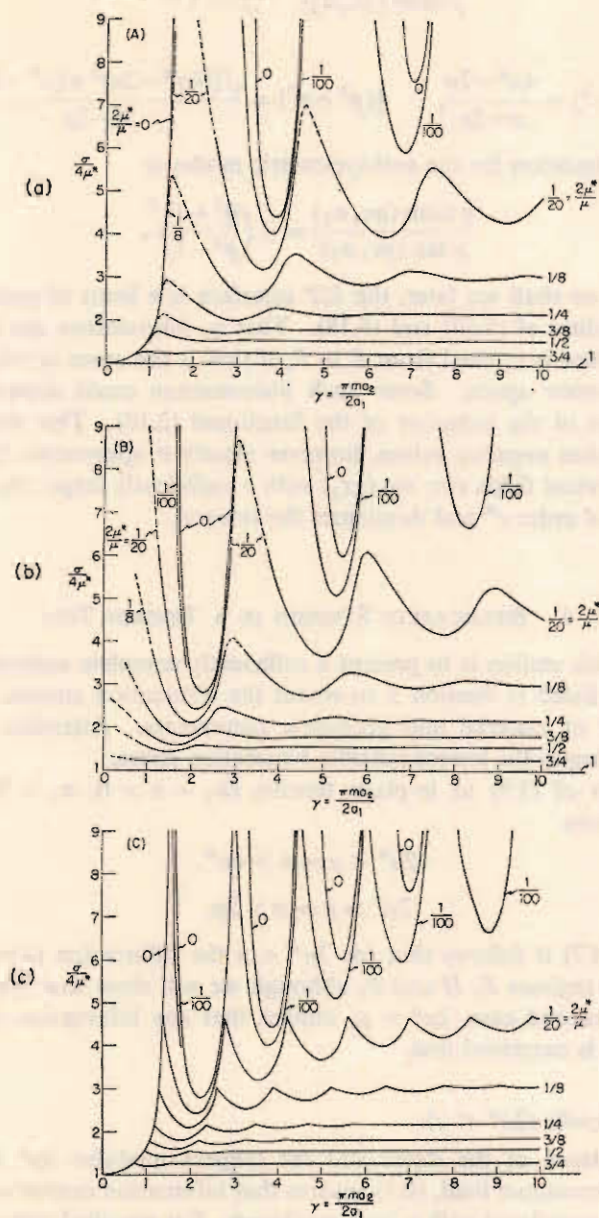


FIG. 2. Lowest bifurcation stresses for $2\mu^*/\mu < 1$: (a) symmetric modes, (b) anti-symmetric modes, and (c) symmetric and anti-symmetric modes.

was used which provided $\sigma/4\mu^*$ to six significant figures. First, the relevant part of the E -regime,

$$1 < \frac{\sigma}{4\mu^*} < \sqrt{\left(\frac{\mu}{\mu^*} - 1\right)},$$

was searched using (5.11) for the symmetric and anti-symmetric modes, respectively. If an eigenvalue was not found, the search was extended into H , i.e.

$$\sqrt{\left(\frac{\mu}{\mu^*} - 1\right)} < \frac{\sigma}{4\mu^*} < \frac{\mu}{2\mu^*}$$

using (5.13) and/or (5.15). In Figs. 2(a, b), values of $\sigma/4\mu^*$ falling in E are shown as solid-line curves while dashed portions are in H . The search need never be taken into P since an infinite set of eigenvalues lies on the H side of the H/P boundary, as will be explained later in Section 6.3.

Included in Figs. 2(a, b) are the limiting solutions to (5.11) for $\mu^*/\mu \rightarrow 0$:

$$\frac{\sigma}{4\mu^*} = \frac{1}{2} \pm \frac{\gamma}{\sin(2\gamma)}, \quad (6.4)$$

where the (+) and (-) go with the symmetric and anti-symmetric modes, respectively. Equations (6.4) can be derived directly taking the specimen to be rigid in shear ($\mu = \infty$) from the start as discussed in Appendix A1. For the special choice $m = 2$, corresponding to artificially enforced symmetry with respect to the midpoint between the ends, (6.4) was given by COWPER and ONAT (1962). The limiting process leading to (6.4) from (5.11) is discussed in Section 6.2.

We have already mentioned that, in H , localized shear layers are in competition with the modes considered in the derivation of (5.13) and (5.15). Where the shear layers are compatible with the boundary conditions, they may lead to bifurcation stresses lower than predicted by (5.13) and (5.15). However, when both symmetric and anti-symmetric modes are taken together the lowest bifurcation stress is always in E . Nevertheless, in some instances shear layers may be associated with stresses only slightly above the lowest bifurcation stress and there is the possibility that they become the final failure mode. A shear-layer analysis is given in Appendix AII.

Figure 2(c) shows curves of the lowest eigenvalue $\sigma/4\mu^*$ as a function of γ when the results for the symmetric and anti-symmetric modes are thrown into competition. A comparison of Fig. 2(c) with Figs. 2(a, b) reveals that the first segment of each festooned curve, as γ increases from zero, is always associated with symmetric bifurcation and the second with an anti-symmetric mode; subsequent segments alternate between symmetric and anti-symmetric modes.

It is now useful to note that the left-hand side of the elliptic eigenvalue equations (5.11) vanishes as $\gamma \rightarrow \infty$ due to the presence of $\sinh(2q\gamma)$ in the denominator (p and q remain finite). Thus, for both symmetric and anti-symmetric modes, the bifurcation stress for $\gamma \rightarrow \infty$ is given by the condition that the numerator on the right-hand side of (5.11) vanishes, i.e.

$$\frac{\sigma}{4\mu^*} = 1 + \frac{\sigma}{4\mu^*} \sqrt{\left(\frac{2\mu - \sigma}{2\mu + \sigma}\right)}. \quad (6.5)$$

This relation is plotted in Fig. 3. The trend towards the limiting values for large γ can be seen in the numerical results of Fig. 2.

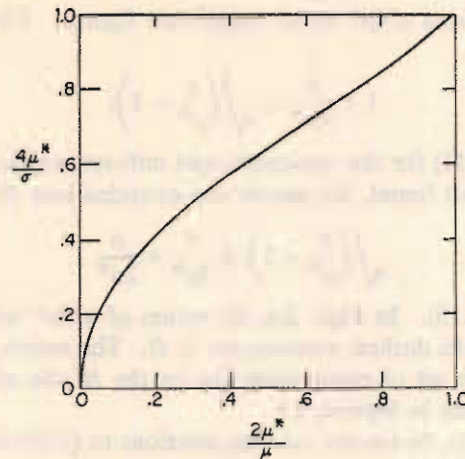


FIG. 3. Lowest bifurcation stress for the limiting case $\gamma \rightarrow \infty$ from (6.5).

The left-hand side of (5.11) also vanishes at all values of γ given by

$$\gamma = j\pi/2p, \quad j = 1, 2, 3, \dots \quad (6.6)$$

The value of $\sigma/4\mu^*$ given by (6.5) is therefore attained for both symmetric and anti-symmetric modes at these values of γ , where, of course, p is computed using the same value of $\sigma/4\mu^*$ in (5.12). As seen in Fig. 2(c) the values of γ given by (6.6) are the points of transition between segments associated with symmetric and anti-symmetric modes. The lowest eigenvalue $\sigma/4\mu^*$ at any value of γ is never greater than (6.5). Since (6.5) is in E , it immediately follows that the lowest bifurcation stress always lies in E when $2\mu^* < \mu$.

The difference between $\sigma/4\mu^*$ at any γ on a curve segment in Fig. 2(c) and the upper-bound value (6.5) diminishes steadily as segments farther and farther from $\gamma = 0$ are considered. It is evident from Fig. 2(c) that the lowest bifurcation stress for a given geometry ratio $\pi a_2/2a_1$ is always associated with $m = 1$. Exceptionally, if $\pi a_2/2a_1 = k\pi/2p$ for any integer value of k then the bifurcation stress is (6.5) and *all* values of m are simultaneously available, including modes with arbitrarily short wavelengths.

6.2 Asymptotic formulae ($2\mu^* < \mu$)

For sufficiently small γ the bifurcation mode is symmetric. The result of a relatively straightforward asymptotic expansion of (5.11) for small γ is

$$\frac{\sigma}{4\mu^*} = 1 + \frac{1}{3}\gamma^2 + \frac{7}{45}\gamma^4 + \mathcal{O}(\gamma^6, \gamma^6\mu^*/\mu). \quad (6.7)$$

The ratio of the tangent modulus to the shear modulus, $4\mu^*/\mu$, first appears in the expansion only in the term of order γ^6 . Up to and including terms of order γ^4 , (6.7) is identical to a similar expansion of (6.4₁). In fact, on the scale of Fig. 2 the difference between the result for infinite shear rigidity ($\mu^*/\mu = 0$) and the curves for $2\mu^*/\mu \leq 1/2$, say, is virtually undetectable if $\gamma < 1$.

The connection between the simple formula (6.4) and the results for a finite shear stiffness is brought out even more clearly by calculating the lowest order influence of a large but finite shear modulus μ on the bifurcation stress. The fairly delicate (and lengthy) process of expanding the eigenvalue equation (5.11₁) for the symmetric modes in small values of μ^*/μ at fixed, finite values of γ gives

$$\frac{\sigma}{4\mu^*} = \frac{1}{2} + \frac{\gamma}{\sin 2\gamma} \frac{2\mu^*}{\mu} \left\{ \left(\frac{\gamma}{\sin 2\gamma} \right)^3 (1 + \cos 2\gamma) - \frac{1}{8} - \frac{\gamma}{\sin 2\gamma} \left(\frac{1}{4} + \frac{1}{3}\gamma^2 \right) \right\} + \mathcal{O} \left(\frac{\mu^*}{\mu} \right)^2. \quad (6.8)$$

For $\mu^*/\mu \rightarrow 0$, (6.8) obviously becomes the limiting equation (6.4). Furthermore, for small γ the terms in the brackets multiplying $2\mu^*/\mu$ can be shown to be of order γ^6 , as required for consistency with (6.7).

Next consider the other extreme of the range of $2\mu^*/\mu$ under present consideration where $2\mu^*/\mu = 1 - \delta$ with $0 < \delta \ll 1$. It is readily shown using (6.5) that, for the limiting case $\gamma \rightarrow \infty$,

$$\frac{\sigma}{4\mu^*} = 1 + \delta + \mathcal{O}(\delta^2) \quad \text{with } q \approx p/\sqrt{3} \approx 1/(2\sqrt{\delta}). \quad (6.9)$$

The relations (6.9) continue to hold for any fixed, finite γ for sufficiently small δ since as $\delta \rightarrow 0$ the left-hand side of (5.11) becomes exponentially small. As can be seen in Fig. 2 and from (6.9), the lowest bifurcation stress just slightly exceeds the stress at maximum load for all values of γ when $2\mu^*/\mu$ is close to unity.

6.3 Eigenvalues in the parabolic regime ($2\mu^* > \mu$)

As remarked in connection with (6.2), $2\mu^* > \mu$ implies $\sigma > 2\mu$ with σ in P . The key to discovering the eigenvalues in this regime is the behavior of p and q for values of $\sigma/2\mu$ only slightly greater than unity. Using their definitions in (5.17) one finds for small positive $\sigma/2\mu - 1$ that

$$p \approx 2 \sqrt{\frac{2\mu^* - \mu}{\sigma - 2\mu}}, \quad q \approx \sqrt{\frac{\mu}{2\mu^* - \mu}}. \quad (6.10)$$

The right-hand side of (5.16) for the symmetric modes becomes

$$\left(\frac{1+q^2}{p^2-1} \right)^2 \approx \left(\frac{\mu^*(\sigma-2\mu)}{2(2\mu^*-\mu)^2} \right)^2 \quad (6.11)$$

and is depicted schematically in Fig. 4.

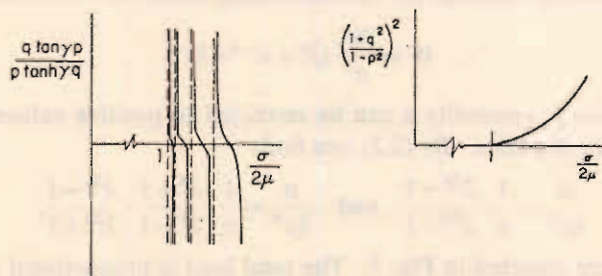


FIG. 4. Schematic sketch of the properties of the parabolic eigenvalue equation (5.16).

Now consider the left-hand side of (5.16). For any fixed non-zero value of γ , $\gamma p \rightarrow \infty$ as $\sigma \rightarrow 2\mu$ from above as seen from (6.10). Because of the presence of $\tan(\gamma p)$ in its numerator, the left-hand side of (5.16) oscillates between $\pm \infty$ in an infinite sequence of intervals bounded below by $\sigma = 2\mu$, as depicted in Fig. 4. It follows that in any finite interval closed below by $\sigma = 2\mu$ there is an infinite sequence of eigenvalues. One can easily show that the value $\sigma = 2\mu$ on the E/P boundary cannot be an eigenvalue itself but is a *point of accumulation*. The E/P boundary plays the same role for the anti-symmetric eigenvalues. A somewhat similar spectrum of eigenvalues was found by BIOT (1965, pp. 194–203) for the problem arising from the compressive loading of a rectangular block between smooth rigid plates. A more detailed discussion of this problem is continued in Appendix AIII.

For the tension problem at hand, bifurcation will be possible as soon as σ exceeds 2μ when $2\mu^* > \mu$, and thus there will always be an infinite set of bifurcation stresses below the stress at maximum load. The associated spectrum of modes includes modes with vanishingly short wavelengths as remarked on in Section 5.3.

Similar considerations reveal that each point on the H/P interface is a point of accumulation when $2\mu^* < \mu$. An infinite sequence of eigenvalues is encountered as $\sigma \rightarrow 2\mu$ from below. In this case there are isolated points on the H/P interface which are themselves associated with eigenvalues.

7. DISCUSSION

(i) We have remarked that the Mooney–Rivlin material is incrementally isotropic under in-plane tension (i.e. $\mu^* = \mu$). If bifurcation occurred it would necessarily be in the parabolic regime when σ exceeds 2μ . But the constitutive relation itself excludes this possibility (cf. (2.2)) and it follows that bifurcation is never possible under plane tension for the boundary conditions considered.

We have also remarked that an initially isotropic, incompressible, finitely-elastic material as in (2.2) can never penetrate the parabolic regime in plane tension. Thus, if bifurcation occurs it will necessarily take place at a stress above that at a load maximum, i.e. $\sigma > 4\mu^*$. Obviously, if no such maximum exists, bifurcation is excluded. On the other hand, the existence of a maximum load point by no means ensures that a bifurcation stress will be reached. Whether or not one will actually be attained depends on the evolution of $\sigma/4\mu^*$, $2\mu^*/\mu$ and a_2/a_1 beyond the load maximum.

As an illustration consider the following generalization of the Mooney–Rivlin material whose energy function for incompressible, plane deformations is

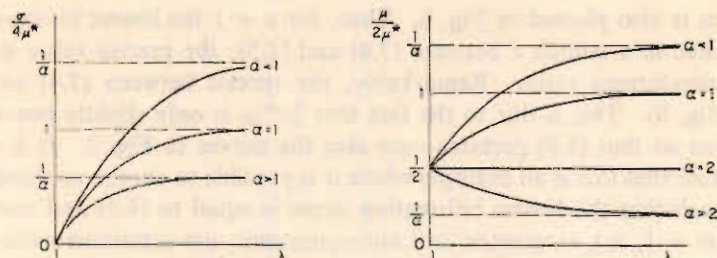
$$W = \frac{2\mu_0}{\alpha^2} (\lambda^\alpha + \lambda^{-\alpha} - 2) \quad (7.1)$$

where without loss in generality α can be restricted to positive values and μ_0 is the ground-state shear modulus. By (2.2) one finds

$$\frac{\sigma}{4\mu^*} = \frac{1}{\alpha} \cdot \frac{\lambda^{2\alpha} - 1}{\lambda^{2\alpha} + 1} \quad \text{and} \quad \frac{\mu}{2\mu^*} = \frac{1}{\alpha} \cdot \frac{\lambda^4 + 1}{\lambda^4 - 1} \cdot \frac{\lambda^{2\alpha} - 1}{\lambda^{2\alpha} + 1}. \quad (7.2)$$

These relations are depicted in Fig. 5. The total load is proportional to

$$\sigma/\lambda = (2\mu_0/\alpha)(\lambda^{\alpha-1} - \lambda^{-\alpha-1}). \quad (7.3)$$


 FIG. 5. Sketches of the dependence of $\sigma/4\mu^*$ and $\mu/2\mu^*$ on the stretch λ from (7.2).

If $\alpha > 1$, σ never attains $4\mu^*$; but if $\alpha < 1$ the load has a single maximum at the value of λ where $\sigma = 4\mu^*$, namely

$$\lambda = \{(1 + \alpha)/(1 - \alpha)\}^{1/2\alpha}. \quad (7.4)$$

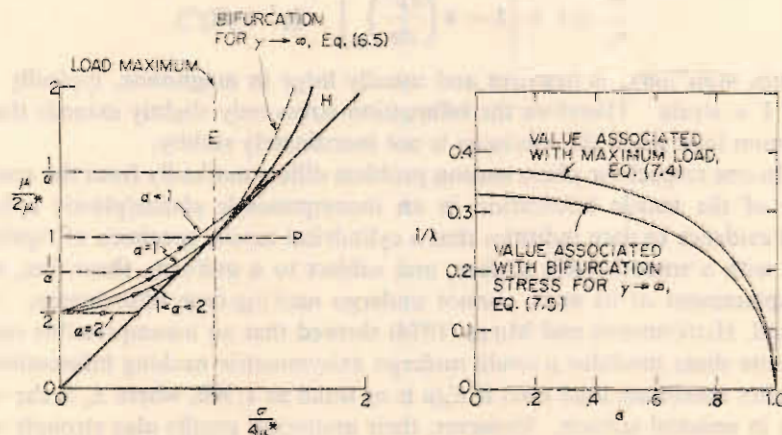
Thereafter the load diminishes monotonically. At the load maximum,

$$\frac{\mu}{2\mu^*} = \frac{\lambda^4 + 1}{\lambda^4 - 1} > 1$$

which falls within E . This can be seen in the evolution of the homogeneous deformations (7.2) in the space of $\mu/2\mu^*$ and $\sigma/4\mu^*$ shown in Fig. 6. The relation (7.4) is plotted on the right in Fig. 6. In the limit $\alpha \rightarrow 0$, equation (7.4) gives $\lambda = e$.

If the specimen is sufficiently slender, bifurcation will occur just following the load maximum as previously discussed. In all cases bifurcation will occur at a stress which does not exceed the limiting value for $\gamma \rightarrow \infty$ in (6.5). Substituting (7.2) into (6.5), one obtains the following equation for the value of λ at which this upper-bound to the bifurcation stress is attained:

$$\frac{\lambda^{2\alpha} - 1}{\lambda^{2\alpha} + 1} \cdot \frac{\lambda^2 - 1}{\lambda^2} = \alpha. \quad (7.5)$$


 FIG. 6. Trajectories of $(\sigma/4\mu^*, \mu/2\mu^*)$. Values of the stretch λ associated with the load maximum and with the upper limit on the bifurcation stress for $\alpha < 1$.

This relation is also plotted in Fig. 6. Thus, for $\alpha < 1$ the lowest bifurcation stress will be reached at a stretch λ between (7.4) and (7.5); the precise value depends on the initial slenderness ratio. Remarkably, the spread between (7.4) and (7.5) is small (see Fig. 6). This is due to the fact that $2\mu^*/\mu$ is only slightly less than unity at bifurcation so that (6.9) pertains—see also the curves in Fig. 2. It is of further interest to note that this is an example where it is possible to choose an initial slenderness ratio such that the lowest bifurcation stress is equal to (6.5) and consequently all modes ($m = 1, \infty$), symmetric and anti-symmetric, are simultaneously available.

(ii) The present analysis applies to incompressible elastic/plastic solids assuming the properties are initially homogeneous and isotropic, or at least orthotropic with respect to the specimen axes. Typically, an initially isotropic metal suffers a monotonic decrease in the ratio of the tangent modulus to the shear modulus on the active plastic loading branch with increasing extension in plane tension. If the yield surface is smooth then, as discussed in Section 2, μ is also the instantaneous modulus for elastic shearing parallel to the specimen axes. Then $4\mu^*/\mu$ may be as small as 1/100 at maximum load. Even if a vertex develops on the yield surface, μ (which is no longer the instantaneous elastic value on the active plastic loading branch) is still likely to be many times $4\mu^*$. Thus, any plane tension specimen with the boundary conditions studied here will undergo a necking bifurcation in the elliptic regime at a stress which is above the stress at maximum load. The total bifurcation mode is some linear combination of fundamental solution increment and eigenmode which ensures that elastic unloading does not occur at bifurcation.

For a relatively slender specimen ($\pi a_2/2a_1 < \frac{1}{2}$, say) the asymptotic formula (6.7) and the rigid/plastic result (6.4) give numerically similar and accurate predictions. If the tangent modulus is a smooth function of σ in the neighborhood of the stress at maximum load, $\sigma_m = 4\mu_m^*$, then (6.7) can be transformed to relate the bifurcation stress explicitly to σ_m . With

$$\mu^* = \mu_m^* + (d\mu^*/d\sigma)_m(\sigma - \sigma_m) + \dots,$$

(6.7) becomes for small γ ,

$$\frac{\sigma}{\sigma_m} = 1 + \left[1 - 4 \left(\frac{d\mu^*}{d\sigma} \right)_m \right]^{-1} \frac{1}{3} \gamma^2 + \mathcal{O}(\gamma^4). \quad (7.6)$$

For metals, $4(d\mu^*/d\sigma)_m$ is negative and usually large in magnitude, typically on the order of 1 ÷ strain. Therefore the bifurcation stress only slightly exceeds the stress at maximum load when the specimen is not inordinately stubby.

(iii) In one respect the plane tension problem differs markedly from the analogous problem of the tensile bifurcation in an incompressible elastic/plastic cylindrical bar. All evidence to date indicates that a cylindrical tensile specimen of rigid/plastic material with a smooth yield surface, and subject to a uniform, shear-free, relative axial displacement of its ends, cannot undergo necking-type bifurcations. On the other hand, HUTCHINSON and MILES (1974) showed that an incompressible specimen with a finite shear modulus μ could undergo axisymmetric necking bifurcations very shortly after maximum load even if E_t/μ is as small as 1/300, where E_t is the tangent modulus in uniaxial tension. However, their numerical results also strongly suggest that, for any finite slenderness ratio, the bifurcation stress becomes unbounded as $E_t/\mu \rightarrow 0$, consistent with the inability of the rigid-plastic specimen to bifurcate.

This point is further emphasized by the asymptotic relation between the bifurcation stress and the slenderness ratio, $\gamma = \pi R/L$ (R and L are the radius and length of the cylinder at bifurcation). For $\gamma \ll 1$,

$$\frac{\sigma}{E_t} = 1 + \frac{\gamma^2}{8} + \frac{\mu}{E_t} \frac{\gamma^4}{192} + \mathcal{O}\left(\gamma^4 \frac{\sigma}{E_t}, \gamma^6 \frac{\mu}{E_t}\right). \quad (7.7)$$

As opposed to the analogous expression (6.7) for the plane problem, coefficients in (7.7) become unbounded as $E_t/\mu \rightarrow 0$.

(iv) An interesting feature of the numerical results of Fig. 2 is the many modes, both symmetric and anti-symmetric, associated with stresses which are, in some instances, only slightly above the lowest bifurcation stress. Included is the possibility of modes with arbitrarily short wavelengths. (For the elastic material (7.1) we have seen that it is actually possible to select an initial slenderness ratio such that an infinite spectrum of modes is associated with the lowest bifurcation stress.) At stresses which may be only slightly higher still, shear bands such as those discussed in Appendix AII become possible. It is not unlikely that some of these higher modes may make their appearance as post-bifurcation or failure modes, rather like the concentrated oblique necking observed in strip tension tests.

ACKNOWLEDGMENT

The work of one of us (J.W.H.) was supported by the United States Air Force Office of Scientific Research under Grant AFOSR-73-2476 and the Advanced Research Projects Agency under Contract DAHC15-73-G-16 and by the Division of Engineering and Applied Physics, Harvard University.

REFERENCES

- | | | |
|---------------------------------------|------|--|
| ARIARATNAM, S. T. and
DUBEY, R. N. | 1969 | <i>Q. appl. Math.</i> 27 , 349. |
| BIOT, M. A. | 1965 | <i>Mechanics of Incremental Deformation</i> . Wiley, New York. |
| COWPER, G. R. and ONAT, E. T. | 1962 | <i>Proceedings of the Fourth U.S. National Congress of Applied Mechanics</i> (University of California, Berkeley; June 18-21, 1962) (edited by ROSENBERG, R. M.), Vol. 2, p. 1023. American Society of Mechanical Engineers, New York. |
| DUBEY, R. N. | 1975 | <i>Thick-body bifurcations of elastic and elastic/plastic solids in plane strain: a correlation study using principal axes technique</i> . Special Publication, Solid Mechanics Division, Waterloo University. In press. |
| HILL, R. | 1958 | <i>J. Mech. Phys. Solids</i> 6 , 236. |
| | 1959 | <i>Ibid.</i> 7 , 209. |
| | 1962 | <i>Ibid.</i> 10 , 1. |
| | 1967 | <i>Ibid.</i> 15 , 371. |
| | 1968 | <i>Ibid.</i> 16 , 229. |
| HUTCHISON, J. W. and
MILES, J. P. | 1974 | <i>Ibid.</i> 22 , 61. |

APPENDIX AI

Rigid/plastic analysis

The constitutive relations (2.1) on the plastic branch are replaced by their normal limit as $\mu \rightarrow \infty$, viz.

$$\frac{\mathcal{D}}{\mathcal{D}t} (\sigma_{11} - \sigma_{22}) = 4\mu^* \varepsilon_{11} = -4\mu^* \varepsilon_{22}, \quad \varepsilon_{12} = 0.$$

From the latter, in place of the fourth-order equation (3.3) for the stream function, we have a standard second-order equation

$$\frac{\partial^2 \psi}{\partial x_1^2} - \frac{\partial^2 \psi}{\partial x_2^2} = 0 \quad (\text{AI.1})$$

at all stress levels, subject to $\partial^2 \psi / \partial x_1 \partial x_2 \geq 0$ for continued loading when $\sigma_1 > \sigma_2$. This is of course hyperbolic, with a single pair of families of characteristics bisecting the coordinate directions.

In the first instance we examine bifurcations for the associated incrementally-linear solid. For the tension problem, with the notation of Section 5, there exist eigenmodes of type

$$\psi = v(x_2) \cos(cx_1), \quad c = m\pi/2a_1, \quad m = 1, 2, \dots, \quad (\text{AI.2})$$

where

$$v'' + c^2 v = 0$$

everywhere. (We recall from (5.5) that previously this had to be satisfied just on the sides.) Such modes have symmetry about the x_1 -axis when $v = \sin(cx_2)$, and then

$$v_1 = c \cos(cx_1) \cos(cx_2), \quad v_2 = c \sin(cx_1) \sin(cx_2). \quad (\text{AI.3})$$

In place of (2.6), therefore, we have

$$\left. \begin{aligned} \dot{n}_{11} - \dot{n}_{22} &= (\sigma - 4\mu^*)c^2 \sin(cx_1) \cos(cx_2), \\ \dot{n}_{12} - \dot{n}_{21} &= \sigma c^2 \cos(cx_1) \sin(cx_2), \end{aligned} \right\} \quad (\text{AI.4})$$

but no longer constitutive relations for \dot{n}_{12} and \dot{n}_{21} separately. In compensation the end-condition $\dot{n}_{12} = 0$ does not now automatically result from the particular choice of ψ , but can be satisfied by taking

$$\dot{n}_{12} = F(x_2) \cos(cx_1). \quad (\text{AI.5})$$

Correspondingly, we take

$$\left. \begin{aligned} \dot{n}_{21} &= G(x_2) \cos(cx_1), \\ F - G &= \sigma c^2 \sin(cx_2), \end{aligned} \right\} \quad (\text{AI.6})$$

where

by (AI.4₂). Then, having regard to (3.1) and (AI.4₁), we have

$$\left. \begin{aligned} \frac{1}{2}(\dot{n}_{11} + \dot{n}_{22}) &= H(x_2) \sin(cx_1), \\ G' + cH &= \frac{1}{2}(4\mu^* - \sigma)c^3 \cos(cx_2), \\ H' - cF &= \frac{1}{2}(4\mu^* - \sigma)c^3 \sin(cx_2). \end{aligned} \right\} \quad (\text{AI.7})$$

Finally, we must satisfy $\dot{n}_{21} = 0$ and $\dot{n}_{11} + \dot{n}_{22} = \dot{n}_{11} - \dot{n}_{22}$ on the sides.

The solution can be carried through in terms of the differential equation and boundary conditions for any one of F , G , and H , but we give all three for completeness:

$$\text{with } \left. \begin{aligned} F'' + c^2 F &= -4\mu^* c^4 \sin(cx_2), \\ F &= \pm \sigma c^2 \sin(ca_2), \quad F' = 4\mu^* c^3 \cos(ca_2) \quad \text{on } x_2 = \pm a_2, \end{aligned} \right\} \quad (\text{AI.8})$$

$$\text{with } \left. \begin{aligned} G'' + c^2 G &= -4\mu^* c^4 \sin(cx_2), \\ G &= 0, \quad G' = (4\mu^* - \sigma)c^3 \cos(ca_2) \quad \text{on } x_2 = \pm a_2, \end{aligned} \right\} \quad (\text{AI.9})$$

$$\text{with } \left. \begin{aligned} H'' + c^2 H &= 4\mu^* c^4 \cos(cx_2), \\ H &= \frac{1}{2}(\sigma - 4\mu^*)c^2 \cos(ca_2), \quad H' = \pm \frac{1}{2}(\sigma + 4\mu^*)c^3 \sin(ca_2) \quad \text{on } x_2 = \pm a_2. \end{aligned} \right\} \quad (\text{AI.10})$$

We thus obtain the eigenvalue equation

$$\frac{\sin(ca_2) \cos(ca_2)}{ca_2} = \frac{2\mu^*}{\sigma - 2\mu^*} \quad (\text{AI.11})$$

in conjunction with the respective solutions

$$F/2\mu^*c^2 = \{1 + ca_2 \tan(ca_2)\} \sin(cx_2) + cx_2 \cos(cx_2), \quad (\text{AI.12})$$

$$G/2\mu^*c^2 = -ca_2 \cot(ca_2) \sin(cx_2) + cx_2 \cos(cx_2), \quad (\text{AI.13})$$

$$H/2\mu^*c^2 = \{ca_2 \cot(2ca_2) - \frac{1}{2}\} \cos(cx_2) + cx_2 \sin(cx_2). \quad (\text{AI.14})$$

It may be noted that the associated stress-rate function is

$$\phi = 2\mu^* \{ca_2 \tan(ca_2) \cos(cx_2) - cx_2 \sin(cx_2)\}$$

as defined in (3.4).

An analysis of this problem by COWPER and ONAT (1962) was based on characteristic coordinates, together with associated fixed-axes components of Cauchy stress-rate. They introduced an assumption corresponding to (3.2), but discarded modes that do not have a transverse axis of symmetry (and in fact considered only the case $m = 2$). However, we see no mathematical reason to reject the mode $m = 1$, for which the eigenstress given by (AI.11) with $c = \pi/2a_1$ is

$$\frac{\sigma}{2\mu^*} = 1 + \frac{\pi a_2/a_1}{\sin(\pi a_2/a_1)}. \quad (\text{AI.15})$$

We have examined the spectrum (AI.11) for all integers m , and find that the least eigenstress is indeed (AI.15) for dimensions such that $a_1/a_2 > 1$. Cowper and Onat also constructed a quite different type of solution when $a_1/a_2 > 2$; this involves a localized necking, but can be activated only by stresses substantially higher even than when $m = 2$.

Analogously to (3.8), a condition that excludes eigenmodes for the incrementally-linear material (and hence also bifurcation in the inhomogeneous problem for the rigid/plastic material) is $\int U dx_1 dx_2 > 0$ for all piecewise-continuously differentiable velocity fields consistent with the constraints and derivable from a stream function satisfying (AI.1). Here, in replacement of (2.10),

$$2U = (\dot{n}_{11} - \dot{n}_{22}) \frac{\partial v_1}{\partial x_1} + (\dot{n}_{12} - \dot{n}_{21}) \frac{\partial v_2}{\partial x_1} = (4\mu^* - \sigma_1 - \sigma_2) \left(\frac{\partial v_1}{\partial x_1} \right)^2 + (\sigma_1 + \sigma_2) \left(\frac{\partial v_2}{\partial x_1} \right)^2.$$

An immediate inference is that, when $0 < \sigma_1 + \sigma_2 < 4\mu^*$, bifurcation cannot occur under any standard boundary-data. For the present tension problem, in particular, the deformation certainly remains homogeneous at least up to maximum load. For velocity fields of type (A1.3), with c as in (A1.2),

$$\iint U dx_1 dx_2 = a_1 a_2 c^4 \left\{ 2\mu^* - (\sigma - 2\mu^*) \frac{\sin(2ca_2)}{2ca_2} \right\}.$$

Since the left-hand side must vanish in an eigenmode, we recover (A1.11).

To obtain the complete solution for *anti-symmetric* modes from equations for symmetric modes, simply replace $\sin(cx_2)$ by $\cos(cx_2)$ and replace $\cos(cx_2)$ by $-\sin(cx_2)$ everywhere, in particular at $x_2 = \pm a_2$. Then (A1.11), which is

$$\frac{\sigma}{2\mu^*} = 1 + \frac{2ca_2}{\sin(2ca_2)}, \quad \text{becomes} \quad \frac{\sigma}{2\mu^*} = 1 - \frac{2ca_2}{\sin(2ca_2)},$$

where $c = m\pi/2a_1$ and $m = 1, 2, \dots$. We can assemble all branches of these two formulae on one diagram (Fig. 7) to furnish the complete spectra for the block under either tension or compression. Cowper and Onat, in dealing with compression, again consider only the anti-symmetric mode $m = 2$.

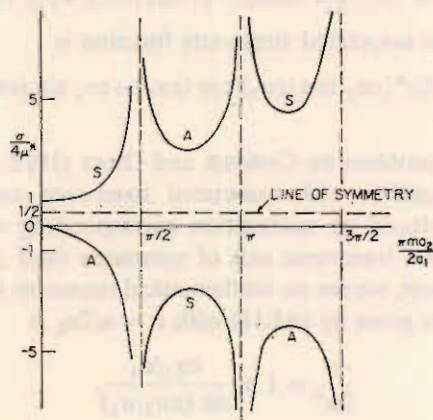


FIG. 7. Bifurcation stresses for a rigid/plastic specimen; S and A denote eigenvalues associated with symmetric and anti-symmetric modes, respectively.

For a rigid/plastic specimen, bifurcation must take place with continuing plastic deformation everywhere in the specimen if the above bifurcation stresses are to hold. A bifurcation mode is some linear combination of the homogeneous solution ($\psi \sim x_1 x_2$) and an eigenmode. For example, in simple tension the form of the symmetric bifurcation modes is

$$\psi = ax_1 x_2 + \cos(cx_1) \sin(cx_2)$$

where $a \geq c^2$ ensures continued loading.

APPENDIX AII

Shear-band bifurcation modes

We have noted that solutions to the field equations exist in the hyperbolic and parabolic regimes of the form $\psi = F(c_1x_1 + c_2x_2)$ where c_1 and c_2 are real and function F is arbitrary. The resulting velocity vector is parallel to, and constant along, the planes $c_1x_1 + c_2x_2 = \text{constant}$, and thus these solutions constitute a shearing field. Here we give a direct shear-band analysis which follows along the lines of HILL's (1962) analysis of acceleration waves in solids.

For a three-dimensional, incompressible, incrementally-linear solid the rate-constitutive law is taken in the form

$$\dot{n}_{ij} = c_{ijkl} \partial v_l / \partial x_k + g \delta_{ij}, \quad (\text{AII.1})$$

where g is undetermined and $\partial v_i / \partial x_i = 0$. Continuing equilibrium requires

$$c_{ijkl} \partial^2 v_l / \partial x_i \partial x_k + \partial g / \partial x_j = 0 \quad (\text{AII.2})$$

where the current state is taken to be homogeneous.

With \mathbf{v} as the unit normal to planes $v_k x_k = \text{constant}$, velocity fields are considered of the type

$$v_i = \eta_i f(v_k x_k) \quad \text{with } v_i \eta_i = 0 \quad (\text{AII.3})$$

and with g as a function of $v_k x_k$ alone. Incompressibility requires orthogonality of \mathbf{v} and $\boldsymbol{\eta}$ corresponding to shearing velocities as depicted in Fig. 8. By (AII.2),

$$C_{ij} \eta_j f'' + v_i g' = 0, \quad (\text{AII.4})$$

where

$$C_{ij} = c_{minj} v_m v_n. \quad (\text{AII.5})$$

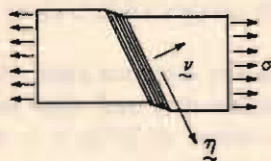


FIG. 8. Shear-band mode.

A trivial homogeneous solution to (AII.4) corresponds to $f'' \equiv 0$ with g constant and \mathbf{v} arbitrary. If $f'' \neq 0$, then the component of (AII.4) on \mathbf{v} implies

$$v_i C_{ij} \eta_j f'' + g' = 0. \quad (\text{AII.6})$$

Elimination of g' from (AII.4) and (AII.6) gives

$$C_{ij} \eta_j = (C_{mn} v_m \eta_n) v_i \quad (\text{AII.7})$$

where the component on $\boldsymbol{\eta}$ is

$$C_{ij} \eta_i \eta_j = 0. \quad (\text{AII.8})$$

The traction-rate on the planes with normal \mathbf{v} is

$$\dot{n}_{ij} v_i = C_{ji} \eta_l f' + g v_j = (v_m C_{ml} \eta_l f' + g) v_j \equiv \dot{n} v_j. \quad (\text{AII.9})$$

From (AII.9) it follows that the traction-rate is normal to these planes with value \dot{n} which is a function of $v_i x_i$. But (AII.6) states that $\dot{n}' = 0$ and therefore \dot{n} is uniform.

Thus, if equations (AII.7) are satisfied by at least one real orthogonal pair $(\mathbf{v}, \boldsymbol{\eta})$, a solution is momentarily possible with vanishing velocity gradients ($f' = 0$) outside some band bounded on each face by a plane $v_k x_k = \text{constant}$ as depicted in Fig. 8. Shearing velocities ($f' \neq 0$) occur within the band. Continuity of traction-rates across the band faces is guaranteed since $\dot{n}_{ij} v_i = \dot{n} v_j$ is everywhere uniform. In general, there is a jump in the components \dot{n}_{ij} across these faces, since $\dot{n}_{ij} \equiv \dot{n} \delta_{ij}$ outside the band. This jump can be related to the quasi-static speed at which the developing shear-band traverses the material as discussed by HILL (1962). A mode such as that depicted in Fig. 8 is the full bifurcation mode in that it is the sum of eigenmodal and homogeneous contributions. Note also that the requirement that the traction-rate vanish on the sides of the specimen is not necessarily satisfied within the band. Strictly speaking, the band at the moment of bifurcation must be vanishingly narrow for a finite-width specimen, and can be regarded as being homogeneously deformed in the limit. The situation is analogous to Hill's 'disc' test, when the rigid platens there are replaced by non-deforming material.

For plane deformations, $\boldsymbol{\eta}$ is fixed in advance according to $(\eta_1, \eta_2) = (v_2, -v_1)$. In terms of the moduli and stresses introduced in the text the non-zero components of c_{ijkl} relevant to plane deformations can be inferred from (2.6):

$$\begin{aligned} c_{1111} &= c_{2222} = 2\mu^* - \frac{1}{2}(\sigma_1 + \sigma_2), \\ c_{1212} &= \mu + \frac{1}{2}(\sigma_1 - \sigma_2), \quad c_{2121} = \mu - \frac{1}{2}(\sigma_1 - \sigma_2), \\ c_{1221} &= c_{2112} = \mu - \frac{1}{2}(\sigma_1 + \sigma_2). \end{aligned}$$

Equation (AII.8) when written out, using $(\eta_1, \eta_2) = (v_2, -v_1)$, is

$$(\mu + \frac{1}{2}\sigma)v_1^4 + 2(2\mu^* - \mu)v_1^2 v_2^2 + (\mu - \frac{1}{2}\sigma)v_2^4 = 0 \quad (\text{AII.10})$$

where $\sigma = \sigma_1 - \sigma_2$. This, of course, is the same consistency equation (4.3) derived before. Satisfaction of (AII.10) ensures (AII.7) since the two components of this equation are not independent.

Shear bands are excluded in the E -regime since (AII.10) has no real solutions. However, in H and P real solutions exist and shear bands are a possibility, as has already been emphasized. For values of $2\mu^*/\mu > 1$, diffuse bifurcation modes are encountered in the rectangular specimen as soon as $\sigma/4\mu^*$ passes into P from E (cf. Section 6.3). Thus, shear-band solutions and diffuse-type modes appear essentially simultaneously. On the other hand, if $2\mu^*/\mu < 1$, then diffuse hyperbolic modes are first encountered at a finite distance into H from the E/H boundary as discussed in connection with Figs. 2(a, b). Shear-band modes are available as soon as the specimen crosses the E/H boundary if a_1/a_2 exceeds v_2/v_1 .

APPENDIX A.III

Notes on Biot's problem

BIOT (1965, pp. 194–203) investigated the problem of a rectangular block, $2a_1 \times 2a_2$, compressed on its sides between smooth rigid plates; its ends are maintained plane by smooth passive constraints. The current stress is homogeneous with $\sigma = \sigma_1 - \sigma_2 > 0$. Boundary data in the eigenmode problem are $v_1 = 0$ and $\dot{n}_{12} = 0$ on the ends and $v_2 = 0$ and $\dot{n}_{21} = 0$ on the sides. We look for eigenmodes

of the form

$$\left. \begin{aligned} \psi &= \cos(c_1 x_1) \cos(c_2 x_2), \\ \text{with } c_1 &= m_1 \pi / 2a_1, \quad c_2 = m_2 \pi / 2a_2, \quad (m_1, m_2) = 1, 2, \dots \end{aligned} \right\} \quad (\text{AIII.1})$$

The block center is at the origin when m_1 and m_2 are odd, but is displaced to $(a_1/m_1, a_2/m_2)$ when m_1 and m_2 are even, etc. All conditions are satisfied since ψ and $\partial^2 \psi / \partial x_1^2$ vanish on the ends, while ψ and $\partial^2 \psi / \partial x_2^2$ vanish on the sides. The differential equation (3.3) is satisfied if

$$\left. \begin{aligned} (\mu + \frac{1}{2}\sigma)c_1^4 + 2(2\mu^* - \mu)c_1^2 c_2^2 + (\mu - \frac{1}{2}\sigma)c_2^4 &= 0 \\ \text{when } \frac{c_1}{c_2} &= \frac{m_1}{m_2} \cdot \frac{a_2}{a_1} \end{aligned} \right\} \quad (\text{AIII.2})$$

For given moduli and block dimensions we can show the spectrum of eigenstresses σ by a simple construction based on Fig. 1. In Fig. 9 denote a general point

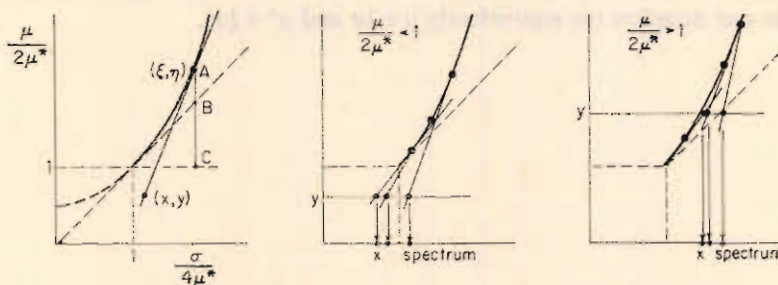


FIG. 9. Graphical construction for eigenvalues in Biot's problem.

$(\sigma/4\mu^*, \mu/2\mu^*)$ by (x, y) and a point on the parabola by (ξ, η) . The equation of the parabola $2\eta = \xi^2 + 1$ can be parametrized as

$$\frac{\eta - \xi}{\eta - 1} = \frac{\eta - 1}{\eta + \xi} = s, \quad \text{say,} \quad (\text{AIII.3})$$

where $0 < s < 1$ on the full arc and $s \leq 0$ on the broken arc. The tangent at (ξ, η) has equation

$$\frac{\xi x}{\eta - 1} - \frac{y}{\eta - 1} = 1$$

which with (AIII.3) can be written as

$$(y + x)s^2 + 2(1 - y)s + (y - x) = 0. \quad (\text{AIII.4})$$

But this is just (AIII.2) if we make the identification

$$s = \left(\frac{m_1}{m_2} \cdot \frac{a_2}{a_1} \right)^2, \quad (\text{AIII.5})$$

so restricting (ξ, η) to the full arc. Notice that only one tangent can be drawn to this arc from any point in regime P but two tangents can be drawn from any point in regime H .

Accordingly, for given a_1/a_2 , we can imagine the dense set of points (AIII.5) along the full arc, for all positive rationals $m_1/m_2 < a_1/a_2$. Specifically, each value of s is associated with a point (ξ, η) by means of $s = BA/CA$ (Fig. 9), the left-hand ratio

in (AIII.3). Tangents are imagined drawn from this set of points to intersect the horizontal line at given $y = \mu/2\mu^*$. The corresponding abscissae form an everywhere dense, countable, spectrum of eigenvalues $x = \sigma/4\mu^*$ extending to infinity.

When $\mu/2\mu^* \leq 1$, the spectrum lies entirely in regime P , and its greatest lower-bound falls on the E/P interface. When $\mu/2\mu^* > 1$, the spectrum lies partly in regime H and partly in regime P , and its greatest lower-bound falls on the E/H interface (for particular dimensions and moduli the interfacial point is itself an eigenstate). Put otherwise: eigenmodes are not found in regime E , namely at stress differences below

$$2\mu \text{ when } \mu \leq 2\mu^* \quad \text{or} \quad 4\mu^* \sqrt{\left(\frac{\mu}{\mu^*} - 1\right)} \text{ when } \mu > 2\mu^*,$$

but are generated if these critical values are exceeded, by however little.

Biot's discussion of (AIII.2) runs on different lines and is mainly for the case $\mu < 2\mu^*$. Note that he holds fixed certain moduli that correspond to $\mu + \frac{1}{2}\sigma$ and $2\mu^* - \mu$ in our notation (or equivalently $\mu + \frac{1}{2}\sigma$ and $\mu^* + \frac{1}{4}\sigma$).